[23]E. Pietarinen and C. P. Knudsen, Nucl. Phys. B57, 637 (1973).
[24]J. K. Kim, Phys. Rev. Lett. 19, 1074 (1967).
[25]As a test, we have calculated the integrals along $\bar{\nu} \leq \nu \leq \nu_0$ of (2.15) and (2.16) using the K-matrix formalism and the results of Ref. 24. At $t \simeq -0.2$ the results are very close to those obtained by resonance saturation. At $t \simeq -0.5$ there is some difference.
[26]V. Barger, K. Geer and F. Halzen, Nucl. Phys. B49, 302 (1972).
[27]J. P. Harnad, Ph.D. thesis, Oxford University, 1973 (unpublished).
[28]The approximate relations (3.4) and (3.5) can be understood by the fact that the FESR for $A^{(\pm)}$ are well satisfied for most t. This point is discussed in Ref. 12 and in the second paper of Ref. 5.
[29]G. Girardi, C. Godreche, and H. Navelet, Nucl. Phys. B76, 541 (1974).
[30]F. Elvekjaer and B. R. Martin, Nucl. Phys. B75, 388 (1974).
[31]P. Astbury *et al.*, Phys. Lett. 23, 2396 (1966).
[32]A. Firestone *et al.*, Phys. Rev. Lett. 25, 958 (1970).
[33]D. Cline *et al.*, Nucl. Phys. B22, 247 (1970).

PHYSICAL REVIEW D VOLUME 10, NUMBER 7 1 OCTOBER 1974

Global description of $0^-\frac{1}{2}^+ \to 0^-\frac{1}{2}^+$ reactions utilizing the bare Pomeron*

N. F. Bali
Physics Department, University of Washington, Seattle, Washington 98195

Jan W. Dash
High Energy Physics Division, Argonne National Laboratory, Argonne, Illinois 60439
(Received 4 March 1974)

It is shown that the combination of a "bare Pomeron" with intercept $\hat{\alpha}_P(0) = 0.85$ in conjunction with a reasonable set of secondary Regge trajectories and a canonical absorption prescription is capable of providing a good global fit to practically all $0^-\frac{1}{2}^+ \to 0^-\frac{1}{2}^+$ meson-nucleon scattering data up to lab momenta of 30 GeV/c. The bare Pomeron with intercept lower than 1 has a large real part which greatly facilitates the description of the data. At higher energies, "renormalization" effects can be expected to be important as inelastic diffraction events, and these lead to a renormalized Pomeron intercept very close to or equal to one. The value $\hat{\alpha}_P(0) = 0.85$ used throughout this intermediate-energy fit is in agreement with current inclusive triple-Regge data and maximum-rapidity-gap distributions. It is also in agreement with certain strong-coupling ABFST (Amati-Bertocchi-Fubini-Stanghellini-Tonin) multiperipheral model calculations. For secondary effects, we have used a family of vector Regge trajectories (ρ, ω, K^*) with a degenerate intercept of about 0.45, and tensor trajectories (A_2, K^{**}) with an intercept of about 0.25. A second vacuum pole emerges with intercept close to 0. The P' (f) trajectory, not included here, can perhaps be expected to appear in conjunction with the renormalization of the Pomeron. Although no wrong-signature nonsense zeros are included in the parametrization, the ρ-A_2 and K^*-K^{**} *pole* couplings are nevertheless very nearly exchange degenerate. SU(3) is used to relate most of the other couplings. The (pole + cut) helicity-flip ρ-A_2 and K^*-K^{**} amplitudes also show considerable exchange-degenerate characteristics. We have used a standard absorption prescription to calculate the second-order bare Pomeron ($\hat{P}$)$\otimes$Reggeon cuts and $\hat{P}\otimes\hat{P}$ cuts. An unusual result emerges—the "enhancement" λ_i factors for all cuts are less than one. This indicates the presence of higher-order cuts which thus dominate over inelastic intermediate-state production in this approach. The data used in this fit are a representative selection of $0^-\frac{1}{2}^+ \to 0^-\frac{1}{2}^+$ data (including πN amplitude analysis, hypercharge-exchange differential cross sections and polarizations; $\pi^\pm p$ and $K^\pm p$ total and differential cross sections, polarizations, and $t = 0$ real-to-imaginary ratios; and πN and KN charge-exchange differential cross sections and polarizations) up to $p_{\rm lab} = 30$ GeV/c and $|t| = 1.5$ (GeV/c)^2.

I. INTRODUCTION

A universal feature of all phenomenological Regge descriptions of two-body scattering data of the last ten years has been the use of a vacuum pole trajectory with intercept of (or very close to) 1.0, and a finite slope. This particular choice has been traditionally suggested by the near constancy of the total and elastic cross sections and the behavior of the real-to-imaginary ratios of the forward elastic amplitudes. Thus, a simple Pomeron pole with intercept at 1, together with a restricted set of leading secondary trajectories and supplemented by an absorption prescription for generating cuts, has been effective in describing differential and total cross sections and some features of the elastic polarizations and forward real-to-imaginary ratios. However, these approaches have never been entirely successful.[1] Certain troublesome features not easily cast in this rather restrictive mold exist. Typical of these have been the difficulties with charge- and hypercharge-exchange reactions, line-reversed reactions, and the shrinking of the diffraction peak at high t.

Many attempts have been made to remedy these difficulties. These attempts have focused on complicating one or another of the inputs to the simple absorption model with exchange-degenerate secondaries and a simple Pomeron pole at one. One approach, similar to ours in spirit, is to change the nature of diffraction to some phenomenological form suggested by the data themselves[2] or by, e.g., an optical model.[3] This enables the absorptive cuts to be rotated in a manner which must otherwise be done by hand,[4] and which appears crucial to the fitting of certain data. Another approach is to neglect any explicit parametrization of cuts but modify the input secondary poles, e.g., by making them complex[5] or including nonleading poles.[6] Another approach[7] gives up all hope of directly connecting J-plane physics with phenomenology and concentrates on duality instead, making assumptions for the imaginary parts of amplitudes through assumptions about the residue structure of s-channel resonances. In this approach the real parts are *a priori* determinable through dispersion relations, but the most complete phenomenology[8] has been done without this constraint, at least for the helicity nonflip amplitude. A final approach, including nonleading Reggeon-Reggeon cuts possibly combined with nonleading poles, is certainly conceivable, but due to a high degree of ambiguity seems unattractive.

The most complete treatment of two-body scattering of any approach has been carried out by Hartley and Kane,[2] hereafter called HK. HK introduce a phenomenological Pomeron which is more complicated than a pole—indeed it has an essential singularity at $J=1$ for $t\neq 0$. Its main feature lies in its substantial real part at $t\neq 0$ which allows a successful "global" fit to all the $0^-\frac{1}{2}^+ \to 0^-\frac{1}{2}^+$ data. This is achieved with a certain breaking of exchange degeneracy, but without an insulting number of free parameters. The phenomenological Pomeron of HK has some theoretical justification in terms of s-channel unitarity, mainly concerning its t dependence at fixed s.[9]

In this paper we shall take a somewhat different viewpoint. Following Chew[10] we shall argue on s-channel unitarity grounds that the energy dependence arising from a probably greatly complicated set of leading J-plane singularities in the usual Froissart-Gribov positive-signatured partial-wave amplitude A_J can be well described, at least for intermediate energies ($p_{\rm lab} \lesssim 30$ GeV/c), by the energy dependence due to an isolated pole in an auxiliary partial-wave amplitude $\hat{A}_J$, whose intercept lies substantially below one. This singularity in $\hat{A}_J$ which we call the "bare Pomeron" ($\hat{P}$) is then responsible for the leading behavior of the full isoscalar amplitude $M^{I=0}(s,t)$ at intermediate energies, and as such enters into the absorptive corrections of the model, which are taken here as $\hat{P}\otimes\hat{P}$ and $\hat{P}\otimes R$ cuts. As the bare Pomeron intercept we use in this fit has an intercept of 0.85, it naturally has a sizable real part even at $t=0$, and thus achieves most of the phenomenological objectives of HK's Pomeron in an economical way. *Furthermore, there is a direct connection of our parametrization of diffraction in two body phenomenology with multiparticle physics.*[11-14] This, in our view, is the most significant point of our approach.

In this paper we present a global fit in the same spirit as HK's fit to most of the $0^-\frac{1}{2}^+ \to 0^-\frac{1}{2}^+$ data, and we show that a quite successful description is possible within the framework of this model.[15] We of course make no claims to the uniqueness of our fit, and therefore, the only inference we can draw from it is that the scheme as proposed is indeed one of the (perhaps) many different ways of accounting semiquantitatively for the same experimental information. However, the fact that the fit seems to be a fairly graceful one, without too many outrageous features, and the fact that it does have some theoretical underpinnings encourage us to believe that there may be some truth buried in it.

Section II of this paper contains a brief theoretical discussion of our model and Sec. III describes the parametrization used. Section IV is devoted to a discussion of the results with emphasis on the amplitudes obtained. Our conclusions are contained in Sec. V. Details of the formulas and the values of the parameters are consigned to the Appendix.

II. THEORETICAL MOTIVATION

The approach taken in this paper is based on the generalized two-component multifireball models for high-energy scattering proposed by Chew,[10] Ter-Martirosyan,[16] and others, but taking into account the results obtained by one of us in the study of inclusive reactions,[11] maximum rapidity gap distributions,[12] and modified ABFST (Amati-

Bertocchi-Fubini-Stanghellini-Tonin) models.[13,14] The discussion centers on unitarity and the consequent connection between two-body processes and inelastic processes. We shall assume that inelastic processes up to intermediate energies ($p_{lab} \lesssim 30$ GeV/c) are dominated by events with no large rapidity gaps (NLRG) in the distribution of their secondaries. Thus elastic and quasielastic processes are not to be included in σ_{inel}. Through unitarity these inelastic events give rise to a total NLRG (single fireball) cross section σ_{sf} which is taken to have a leading power behavior of the form $(s/s_0)^{\hat{\alpha}_P(0)-1}$, where $\hat{\alpha}_P(0)<1$ is the intercept of what we shall call the unrenormalized or bare Pomeron. If one uses a multiperipheral model[13,14] for σ_{sf}, this leading power dependence has no logarithms, and its coefficient factorizes.

To describe the next leading term in σ_{sf} one must assume the existence of unitary absorptive corrections to the multiperipheral production amplitudes which were used as the mechanism for generating the $\hat{P}$.[17] These corrections do not affect the $\hat{P}$ pole, but instead affect the $\hat{P}\times\hat{P}$ cut. In principle, they are responsible for changing the sign of the $\hat{P}\times\hat{P}$ cut from its positive value in the unabsorbed multiperipheral calculation to negative, as required by t-channel unitarity. Without explicitly treating production-amplitude unitarity these corrections cannot be calulated. To the extent that the magnitude of the $\hat{P}\times\hat{P}$ cut is small compared to that of the $\hat{P}$ pole, one may still hope to use the unabsorbed multiperipheral model as a reasonable approximation in performing phenomenology on inelastic processes at intermediate energies, at least at a qualitative level. The results of our two-body phenomenology indicate that the $\hat{P}\times\hat{P}$ cuts are smaller than the $\hat{P}$ pole.

We should mention at this stage that the multiperipheral model we have in mind as a first approximation to σ_{sf} is a multiperipheral subcluster resonance model, the prototype of which is the ABFST strong-coupling resonance model, with phenomenologically determined off-shell behaviors.[13,14] This is a reasonable choice insofar as σ_{sf} has no large rapidity gaps by definition.

At intermediate energies, then, $\sigma_{inel}^{ab}\approx\sigma_{sf}^{ab} \sim\gamma_a\gamma_b s^{\hat{\alpha}_P(0)-1}$ to leading order. The elastic and those quasielastic cross sections where vacuum exchange is possible fall as $s^{2\hat{\alpha}_P(0)-2}$ in this region, and the leading-order behavior of total cross sections is the same as that of the inelastic cross sections.

At energies beyond the intermediate range, some inelastic events begin to develop large rapidity gaps (LRG). Since the subenergy s_i spanning the large rapidity gap is still largely in the intermediate region except at astronomical energies, we can expect that in these diffractive inelastic events the leading subenergy behavior will have the form $(s_i/s_0)^{\hat{\alpha}_P}$.[11] The appearance of these inelastic diffractive LRG events can be expected to modify ("renormalize") the energy behavior of the total inelastic cross section. This renormalization can be studied in a multifireball model with σ_{sf} given by the ABFST resonance model, and indications are that a renormalized Pomeron intercept very close to 1 is consistent with our approach.[11] The parameter Δ defining a large rapidity gap is of course tied up with $\hat{\alpha}_P(0)$, and a determination of the relationship between these quantities rests on examination of inelastic data. A good guess is $\Delta\approx 1.5-2$. In particular our approach implies additional contributions to the diffractive component of the inelastic cross section to those which are easily accessible to experimental analysis.[12] The NAL data are not in contradiction with the presence of a substantial inelastic diffractive cross section, and the plots of maximum-rapidity-gap distributions in fact suggest it.[12]

In J-plane language, we introduce an auxiliary partial-wave amplitude $\hat{A}_J$ which at $t=0$ is the Froissart-Gribov projection of the NLRG (single fireball) cross section. Its leading pole ($\hat{P}$) and cut ($\hat{P}\times\hat{P}$) singularities at $J=\hat{\alpha}_P(t)$ and $J=2\hat{\alpha}_P(t/4)-1$ provide a simple parametrization of the inelastic cross section at intermediate energies, where it is nearly equal to σ_{sf}. If the renormalized singularities present in the usual Froissart-Gribov partial-wave amplitude A_J are used to parametrize the inelastic cross sections at intermediate energies, a complicated set of them must be included. These can involve, e.g., a myriad of complex poles close to $J=1$ (see Ref. 18) and even the full complexity of a Gribov calculus[19] which, if it simplifies at all, does so only at much higher energies.[20] The energy dependence of the sum of these complicated effects at intermediate energies is simply expressed by the energy dependence arising from the leading singularities in $\hat{A}_J$ in our approach.

The process of renormalization of the Pomeron can reasonably be expected to give rise to the P' (f) singularity via the "schizophrenic Pomeron" mechanism.[21] We therefore do not expect to find the f as a singluarity in $\hat{A}_J$, and in fact we do not include the f here, although a vacuum singularity at $J=0$ is included.

As has been discussed by several authors, the acceptable values of $\alpha_P(0)$ [or $\hat{\alpha}_P(0)$] are constrained by inclusive $x\approx 1$ data and the resultant value of the renormalized triple-Pomeron coupling $g_P(t)$ [or the unrenormalized triple-Pomeron coupling $\hat{g}_P(t)$]. Very-high-energy two-body data of course require $\alpha_P(0)\sim 1$. The more usual inclusive parametrizations[22] involve the renormalized Pomeron pole (neglecting cut corrections) and obtain a small renormalized triple-Pomeron coupling. This in turn implies that the bare Pomeron intercept is close to 1. Since triple-Regge subenergies are in intermediate regions even at CERN ISR energies, our philosophy requires the bare Pomeron to be used, along with the bare triple-Pomeron coupling. The latter turns out to be quite large in this approach,[11] and the sizable renormalization effect implied is sufficient to renormalize the bare Pomeron at 0.85 to 0.99 in the ABFST multifireball model.[11]

Further results obtained in strong-coupling ABFST resonance models with off-shell modifications consistent with the intermediate-energy description of certain multiprong inelastic cross sections[13] indicate that $\hat{\alpha}_P(0)=0.85$ is reasonable.[14]

Finally we wish to make some remarks about rising total cross sections at high energies in this approach. Due to the fast falloff of the single-fireball cross section, one cannot simply invoke low-mass diffraction as being responsible for the rise[23]; indeed the whole of the diffractive cross section in model calculations[11] goes into maintaining the total cross section at a constant value at high energies. However, absorptive (renormalized) $P\otimes P$ cuts are then perfectly capable of generating the rise in total cross sections, although the magnitudes of these cuts is at present incalculable, being related to unitarity of the production amplitudes.[17]

We close this section with a simple mathematical illustration of our preceding remarks which should illuminate the discussion. We shall write an elastic amplitude $T_{\rm el}(s,t)$ as an integral over the Sommerfeld-Watson contour in the following manner (see Ref. 12):

$$T_{\rm el}(s,t)=-\int_{c-i\infty}^{c+i\infty}\frac{dj}{2\pi i}\,\frac{(e^{-i\pi/2}s/s_0)^j}{\sin(\pi j/2)}\times\frac{e^{-bj}}{j-\hat{\alpha}(t)-\hat{g}^2(t)\,e^{-bj}}\,. \qquad (1)$$

The parameter b reflects the existence of inelastic diffractive thresholds and $\hat{g}$ is closely related to the triple bare Pomeron coupling. The exponents e^{-bj} follow from the Froissart-Gribov formula. They state the fact that thresholds in $\ln s$ are reflected in the asymptotic behavior in j.

Now, the unrenormalized partial-wave amplitude $\hat{A}_j(t)$ in this simple model is

$$\hat{A}_j(t)=e^{-bj}/[\,j-\hat{\alpha}(t)]\,. \qquad (2)$$

The renormalized partial-wave amplitude $A_j(t)$ is

$$A_j(t)=e^{-bj}/[\,j-\hat{\alpha}(t)-\hat{g}^2(t)\,e^{-bj}]\,. \qquad (3)$$

This can be rewritten as

$$A_j(t)=\frac{e^{-bj}}{j-\hat{\alpha}(t)}\sum_{k=0}^{\infty}\left(\frac{\hat{g}^2e^{-bj}}{j-\hat{\alpha}(t)}\right)^k\,. \qquad (4)$$

Now we can discuss the unrenormalized bare Pomeron $\hat{P}$ and the renormalized Pomeron P. The bare $\hat{P}$ is a pole at $j=\hat{\alpha}(t)$ in $\hat{A}_j(t)$. We should note immediately that $\hat{\alpha}(t)$ is a function of t only. It does not depend on s, and it cannot depend on s, since the s dependence of amplitudes enters through the factor s^j in the Sommerfeld-Watson projection [Eq. (1)]. Therefore the $\hat{P}$ pole at $j=\hat{\alpha}(t)$ in $\hat{A}_j(t)$ is not an energy-dependent pole, and it is not to be thought of as such. The renormalized Pomeron is, strictly speaking, the leading singularity of $A_j(t)$, a different function from $\hat{A}_j(t)$, in Eq. (3). However, if there are other singularities of $A_j(t)$ near $j=1$, at finite energies we will not be able to isolate them from a pole at $j=1$, so that effectively, the renormalized Pomeron will consist of many singularities near $j=1$. Now, we shall evaluate Eq. (1) in two ways. First, we will use the expansion of $A_j(t)$ in Eq. (4). At finite s, because of the exponents in j, only a finite number of terms in Eq. (4) will contribute to the integral in Eq. (1). We first restrict our attention to the intermediate-energy region

$$b<\ln(s/s_0)<2b\,. \qquad (5)$$

We see that, in fact, only the $k=0$ term will contribute to the imaginary part of $T_{\rm el}(s,t)$. This is because for all other terms we can close the contour to the right to get zero. Hence, we obtain for $b<\ln(s/s_0)<2b$, the exact expression

$$\sigma_{\rm tot}=\hat{\beta}(0)\,(s/s_0)^{\hat{\alpha}_0-1}\,, \qquad (6)$$

where $\hat{\beta}(0)=e^{-b\hat{\alpha}_0}/s_0$. The phase of $T_{\rm el}$ in leading order in this region is just that of the bare Pomeron; i.e., for $b<\ln(s/s_0)<2b$

$$T_{\rm el}(s,t)=\frac{-\hat{\beta}(t)}{\sin(\pi\hat{\alpha}/2)}\left(e^{-i\pi/2}\frac{s}{s_0}\right)^{\hat{\alpha}(t)}\,. \qquad (7)$$

[We have had to neglect real terms of $O(\hat{g}^{2k})$ in Eq. (7) coming from the inelastic diffractive amplitudes below their thresholds, but since this is an effect we have no handle on, we neglect it.]

Now we can also evaluate Eq. (1) by simply moving the contour $c\to-\infty$. If we do this, we obtain the expression exact at all s in this model,

$$\sigma_{\rm tot}=\sum_{m=1}^{\infty}\beta_m(0)\,(s/s_0)^{j_m-1}\,, \qquad (8)$$

where j_m is the position of the mth singularity in $A_j(0)$ with residue β_m. (We have neglected logarithms.)

Now we notice several things:

(1) The energy dependence of σ_{tot} expressed using the bare $\hat{P}$ in Eq. (6) is a lot simpler than that using Eq. (8) with the renormalized P in the intermediate-energy region $b < \ln(s/s_0) < 2b$. Setting $b = 2$, a reasonable estimate, leads roughly to the same definition of intermediate energies as used in our fit.

(2) The f does not appear as a singularity of $\hat{A}_j(t)$. In principle it must appear as a singularity of $A_j(t)$ at $j = \alpha_f(t)$. Thus, if one wants to use the f trajectory in performing phenomenology, one must also use the correct renormalized Pomeron. Actually, $\hat{A}_j(t)$ might have included an "unrenormalized f," and in fact we shall employ a vacuum pole at $j = 0$, which will play a minor role in the fit.

(3) At higher energies, $\ln(s/s_0) > 2b$, Eq. (6) is no longer valid, since explicit terms of $O(\hat{g}^{2k})$ enter from the expansion in Eq. (4). Either we must add these in explicitly or else use the exact expression, Eq. (8). We always require $\ln(s/s_0) < 2b$; hence we need not worry about this problem.

(4) Absorptive cuts and secondary $(\rho, \ldots)$ trajectories used in the fit are added in by hand, and have not appeared in our little model above.

III. PARAMETRIZATION AND RESULTS

We now summarize the parametrization used for this fit. The results are given in Tables I and II, and full details are to be found in the Appendix. The slope of the bare Pomeron was determined phenomenologically, and the slopes of the secondary trajectories were fixed at 1 GeV^{-2}. These were taken as SU(3)-degenerate vector (ρ, ω, K^*) and tensor (A_2, K^{**}) trajectories with possible renormalization effects ignored. We also included a low-lying vacuum pole at $J = 0$,[24] which we call P''. The residue functions in all cases were parametrized with simple exponentials and without wrong-signature nonsense zeros. The isoscalar flip amplitudes were set equal to zero. SU(3) was used to relate the contributions of a given secondary pole to all reactions, and two SU(3)-breaking parameters were introduced for the bare Pomeron pole. The cuts used were the simplest possible and are described in the Appendix. They involve two λ factors, which turn out to be less than one. This has the significance of implying the dominance of higher-order cuts over inelastic intermediate-state cuts, neither of which was explicitly included.

In all, our parametrization of the intermediate-energy $0^-\frac{1}{2}^+ \to 0^-\frac{1}{2}^+$ data involves a total of 34 parameters for about 1000 data points, but at least some of these turn out to be highly constrained. The $\hat{P}$ intercept of 0.85 is fixed at the value already used in triple Regge fits.[11] Further, the ρ-A_2 and K^*-K^{**} pole couplings are nearly degenerate, both for helicity flip and helicity nonflip, and the ω coupling is near its SU(3) value relative to the ρ. Effectively, we have 26 independent free parameters, compared to about 20 for HK.[2]

The global fit shown in Figs. 1 to 15 was obtained by a weighted least-squares minimization program. As could be expected, better looking curves could be obtained by doing a "local" fit

TABLE I. SU(3) coefficients [see Eq. (18), Appendix]. In the last two columns $\eta^{(\pm)} = 1 \pm 2F$ and F has two values (nonflip, flip).

i	(Reaction)	$\hat{P}$	P''	ω	ρ	A_2	K^*	K^{**}
1	$\pi^+ p \to \pi^+ p$	$\hat{S}_\pi$	2		-2			
2	$\pi^- p \to \pi^- p$	$\hat{S}_\pi$	2		2			
3	$\pi^- p \to \pi^0 n$				$-2\sqrt{2}$			
4	$\pi^- p \to \eta n$					$2(\frac{2}{3})^{1/2}$		
5	$K^- p \to K^- p$	$\hat{S}_K$	1	1	1	1		
6	$K^+ p \to K^+ p$	$\hat{S}_K$	1	-1	-1	1		
7	$K^- n \to K^- n$	$\hat{S}_K$	1	1	-1	-1		
8	$K^+ n \to K^+ n$	$\hat{S}_K$	1	-1	1	-1		
9	$K^- p \to \bar{K}^0 n$				2	2		
10	$K^+ n \to K^0 p$				-2	2		
11	$K_L^0 p \to K_S^0 p$			-1	1			
12	$\pi^- p \to K^0 \Sigma^0$						$\sqrt{2}\,\eta^{(-)}$	$\sqrt{2}\,\eta^{(-)}$
13	$\pi^+ p \to K^+ \Sigma^+$						$2\eta^{(-)}$	$2\eta^{(-)}$
14	$K^- p \to \pi^- \Sigma^+$						$-2\eta^{(-)}$	$2\eta^{(-)}$
15	$\pi^- p \to K^0 \Lambda$						$-(\frac{2}{3})^{1/2}\eta^{(+)}$	$-(\frac{2}{3})^{1/2}\eta^{(+)}$
16	$K^- n \to \pi^- \Lambda$						$(\frac{2}{3})^{1/2}\eta^{(+)}$	$-(\frac{2}{3})^{1/2}\eta^{(+)}$
17	$K^- p \to \pi^0 \Lambda$						$\eta^{(+)}/\sqrt{3}$	$-\eta^{(+)}/\sqrt{3}$
18	$K^- p \to \eta_8 \Lambda$						$\eta^{(+)}$	$\eta^{(+)}/3$
19	$K^- n \to \eta_8 \Sigma^-$						$-\sqrt{6}\,\eta^{(-)}$	$-(\sqrt{6}/3)\,\eta^{(-)}$

TABLE II. Parameters obtained in the fit.[a]

	α_k^0	α_k'	$\tilde{\beta}_s^k$	$\tilde{\beta}_f^k$	γ_s^k	γ_f^k
$\hat{P}$	0.85	0.304	105.32	0	1.625	
P''	−0.033	1.	93.63	0	3.957	
ω	0.441	1.	61.22	0	5.0	
ρ	0.441	1.	13.02	66.1	5.036	4.024
A_2	0.254	1.	13.42	71.3	6.147	−0.144
K^*	0.441	1.	6.68	57.07	3.514	2.052
K^{**}	0.254	1.	7.84	58.68	0.992	1.57′

[a]Other parameters are $s_0 = 1\ \mathrm{GeV}^2$, $F = \left\{\begin{smallmatrix}1.6342\\0.1766\end{smallmatrix}\right\}$ for $\left\{\begin{smallmatrix}\text{nonflip}\\\text{flip}\end{smallmatrix}\right\}$, $\hat{S}_\pi = 1.383$, $\hat{S}_K = 1.176$, $\lambda_{\hat{P}\pi} = 0.476$, $\lambda_{\hat{P}K} = 0.676$, $\Gamma(\eta \to 2\gamma)/\Gamma(\eta \to \text{all}) = 0.38$.

to a limited subset of the data without great changes in the parameters.

Figure 1 contains the results for the $\pi^\pm p$ and $K^\pm p$ total cross sections[25] and Fig. 2 shows the forward real to imaginary amplitude ratios.[26] The most notable features of these data include the flat shape of $\sigma_{\text{tot}}^{K^+p}$ and the positive K^-p real to imaginary amplitude ratio, both of which are reproduced. Figure 3 contains the 6-GeV/c πN amplitude analysis results.[27] The crossover zero at $t \approx -0.2$ in $\mathrm{Im}M_{++}^{I=1}$ and the "Regge-pole-like" characteristics of the double zero and single zero at $t \approx -0.5$ in $\mathrm{Re}M_{+-}^{I=1}$ and $\mathrm{Im}M_{+-}^{I=1}$ are a consequence of our absorption procedure, as in HK's approach.[2] $\mathrm{Re}M_{++}^{I=1}$ has less absorption due to the $\hat{P}$ than does $\mathrm{Im}M_{++}^{I=1}$ and is therefore less peripheral. Figures 4–7 show the results for the elastic $\pi^\pm p$ (Ref. 28) and $K^\pm p$ (Ref. 29) differential cross sections and polarizations,[30] and the corresponding results[31,32] for $\pi^-p \to \pi^0 n$ and $\pi^-p \to \eta n$ are exhibited in Figs. 8 and 9. All features are satisfactory except for the large-t $\pi^-p \to \pi^0 n$ data. (Slight changes in the global parameters afford a better description of these data; an example is shown by the dashed curves.) The $\pi^-p \to \pi^0 n$ polarization results are good, the absorption model dip at around $t \approx -0.6$ being quite mild here. Figure 10 contains the results for the "rotating" and "real" reactions[33,34] $K^-p \to \bar{K}^0 n$ and

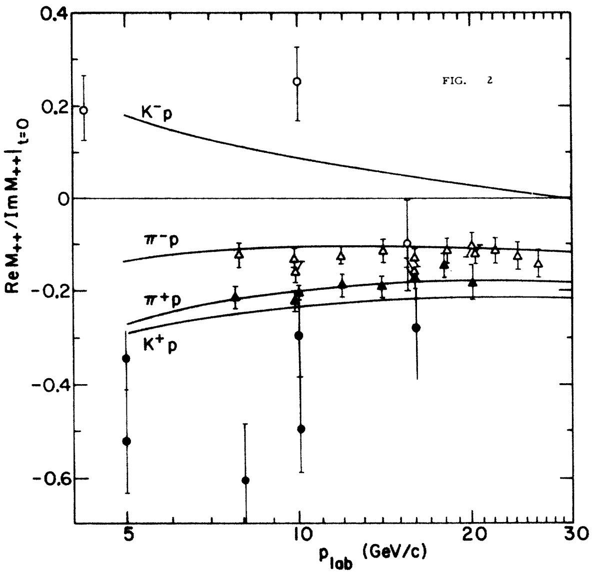

FIG. 2. Real to imaginary amplitude ratios at $t = 0$ for K^-p (open circles), π^-p (open triangles), π^+p (closed triangles), and K^+p (closed circles).

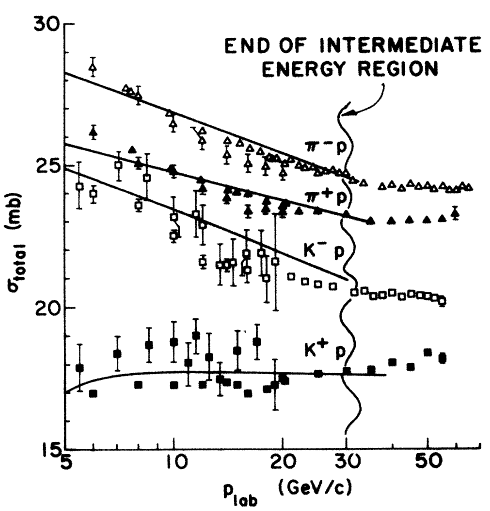

FIG. 1. Total $\pi^\pm p$ and $K^\pm p$ cross sections. The fit is shown only up to $P_{\text{lab}} \sim 30$ GeV/c, which marks the end of the intermediate-energy region in which the fit is expected to be valid.

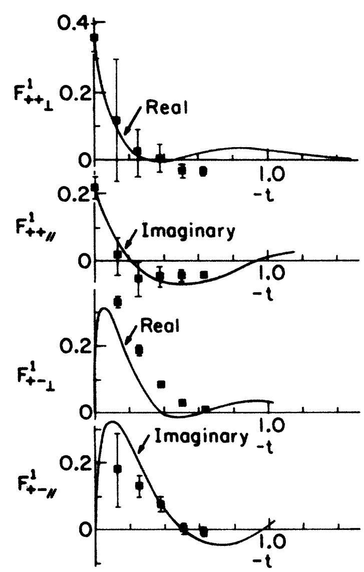

FIG. 3. πN amplitude analysis results at 6 GeV/c. The notation is that of Ref. 27.

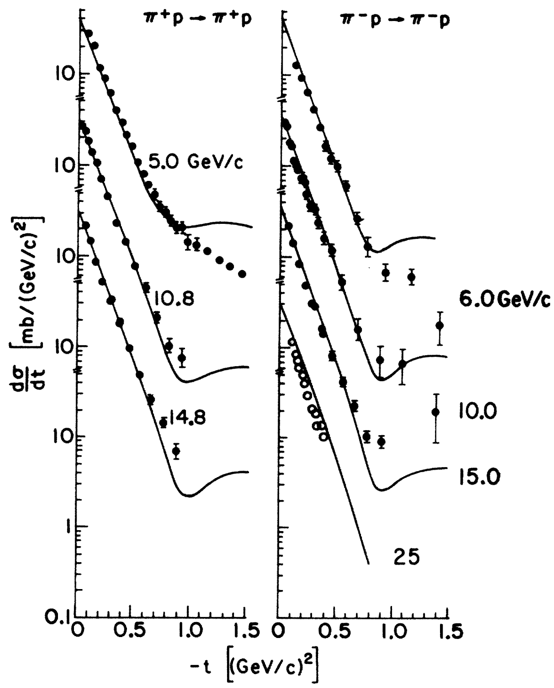

FIG. 4. Elastic $\pi^{\pm}p$ differential cross sections.

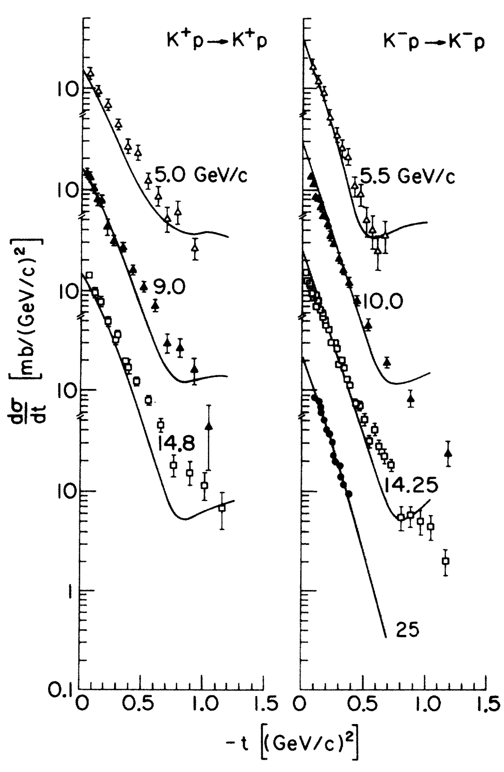

FIG. 5. Elastic $K^{\pm}p$ differential cross sections.

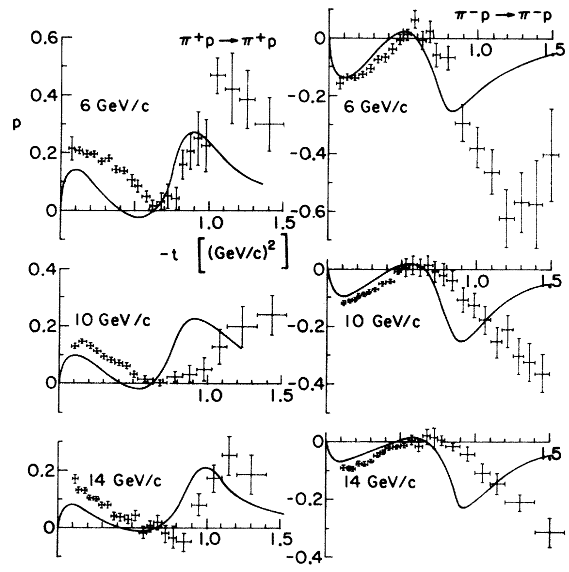

FIG. 6. Elastic $\pi^{\pm}p$ polarizations.

$K^+n \to K^0p$ which are also reasonable, as is the description of the recent $K^-p \to \bar{K}^0n$ polarization data.[35] Figures 12 and 13 show the results for hypercharge-exchange differential cross sections. We have plotted the same hypercharge data as in HK,[36-40] except that more recent experimental low-energy results[41] for $\pi^-p \to K^0\Sigma^0$ and $\pi^-p \to K^0\Lambda^0$ are plotted in Fig. 13(b). The description of the hypercharge polarizations[36,37,39,42] shown in Fig. 14 is adequate. Finally, Fig. 15 shows the description of the reaction $K_L^0p \to K_s^0p$, recently measured at SLAC.[43] Our model is also consistent with these data.

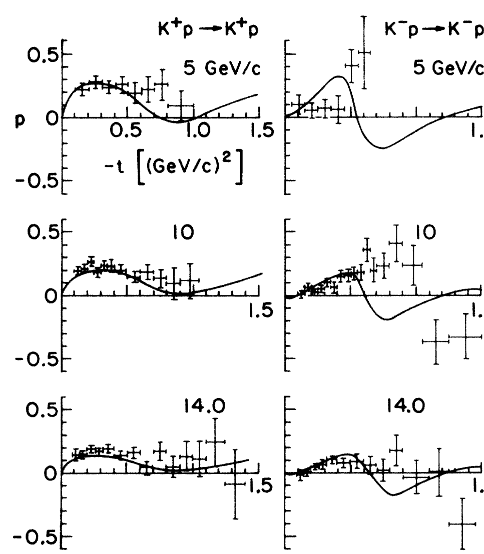

FIG. 7. Elastic $K^{\pm}p$ polarizations.

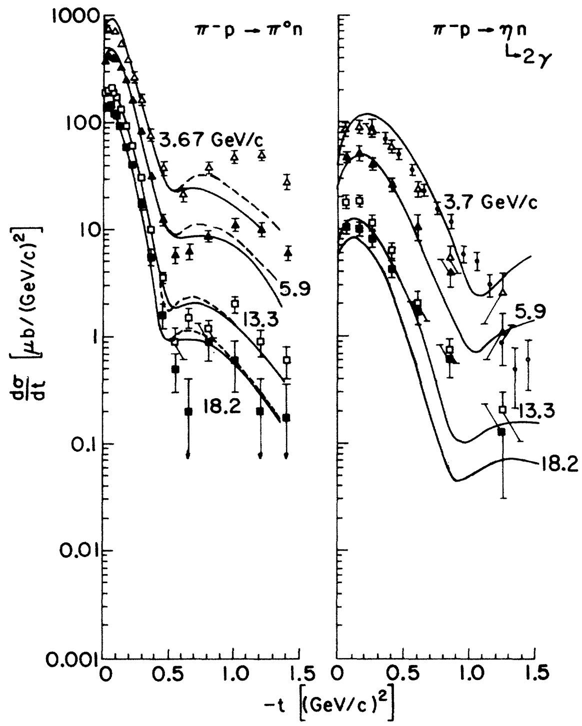

FIG. 8. Differential cross sections for $\pi^- p \rightarrow \pi^0 n$ and $\pi^- p \rightarrow \eta n$. The dashed lines are the results from another global fit with slightly different parameters.

We should mention the motivation for choosing the specific cutoff of 30 GeV/c for the intermediate-energy region. In principle, this should be done by a direct determination of the threshold for appreciable inelastic diffraction effects. While

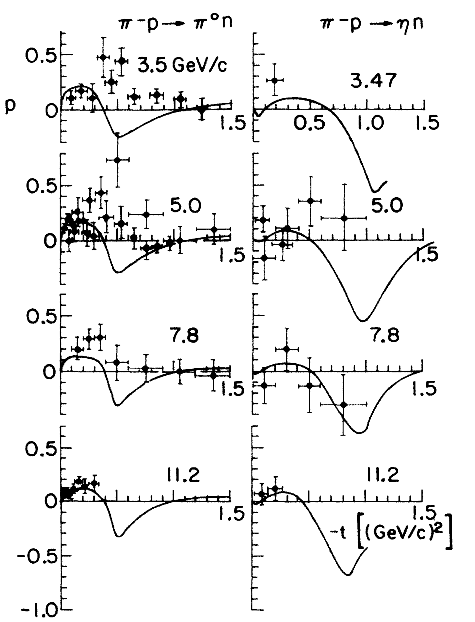

FIG. 9. Polarizations for $\pi^- p \rightarrow \pi^0 n$ and $\pi^- p \rightarrow \eta n$.

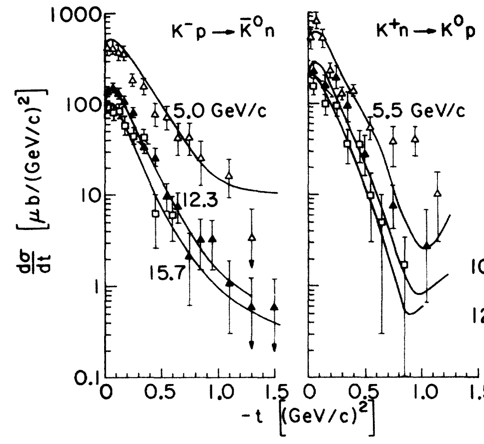

FIG. 10. Differential cross sections for $K^- p \rightarrow \bar{K}^0 n$ and $K^+ n \rightarrow K^0 p$.

30 GeV/c is not an unreasonable *a priori* estimate for such a threshold, our approach here is pragmatic in the sense that above 30 GeV/c our descriptions of total cross sections begin to break down (particularly for $K^+ p$). A further hint is seen in the $t = 0$ real to imaginary ratios. Above 30 GeV/c, these presumably go to zero, whereas our fit shows a slight reverse turnover. To reiterate: Our approach to two-body phenomenology utilizing the bare Pomeron is only valid at intermediate energies ($\lesssim 30$ GeV/c). Above these energies, renormalization effects are expected to become important, leading to constant (or slightly rising) cross sections, etc.

In the next section we shall describe the fit in somewhat more detail, with due attention paid to the amplitudes involved.

IV. DETAILS OF THE AMPLITUDES AND RESULTS

We now analyze some of the more technical points of our results. The isoscalar nonflip $\pi^- p \rightarrow \pi^- p$ amplitudes at 10 GeV/c are shown in Fig. 16. The $\hat{P}$ pole with its sizable real component is used to calculate the absorptive cuts. This leaves open the question of the results that a more ambitious cut scheme would produce in-

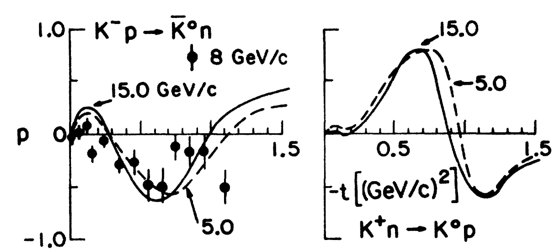

FIG. 11. Polarization results for $K^- p \rightarrow \bar{K}^0 n$ and predictions for $K^+ n \rightarrow K^0 p$.

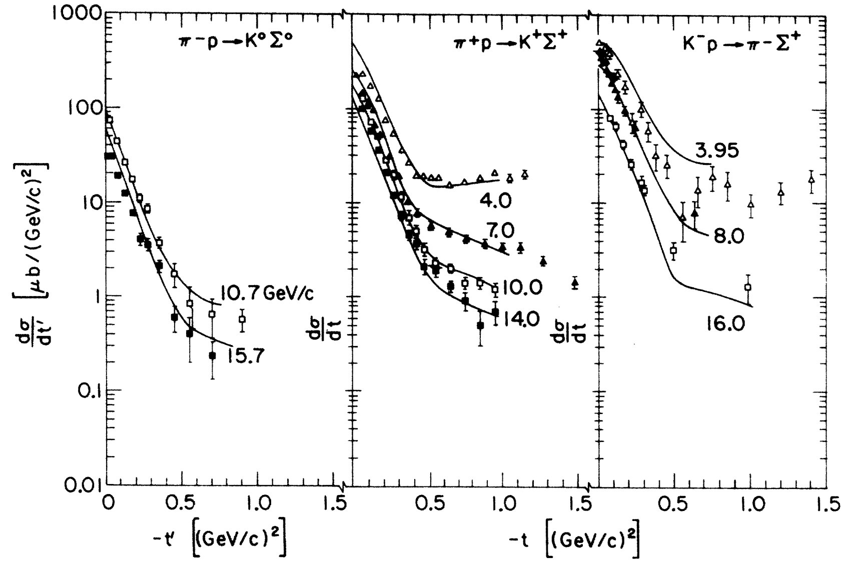

FIG. 12. Hypercharge-exchange differential cross sections: $\pi^- p \to K^0\Sigma^0$, $\pi^+ p \to K^+\Sigma^+$, and $K^- p \to \pi^-\Sigma^+$.

volving absorption with the entire isoscalar amplitude as is the philosophy in HK. Since our λ factors are less than 1, such a scheme should include explicit $\hat{P}\times\hat{P}\times\hat{P}$ cuts in addition to $\hat{P}\times\hat{P}\times R$ cuts. The $\hat{P}\times\hat{P}\times\hat{P}$ cut will partially restore the real part of the $\hat{P}$ pole canceled by the $\hat{P}\times\hat{P}$ cut. In the present description, the $\hat{P}+\hat{P}\times\hat{P}$ amplitude has a relatively flat phase $\approx \pi/2$ as if it were a fixed pole at $J\approx 1$. However, $\mathrm{Re}(\hat{P}+\hat{P}\times\hat{P})$ does have a zero at $t\approx -0.5$. When combined with the single zero of $\mathrm{Im}(\rho+\hat{P}\times\rho)_{+-}$ as evidenced in Fig. 17, this produces a double zero in the elastic $\pi^\pm p$ polarizations (see Fig. 6). The other contributing term $\mathrm{Im}(\hat{P}+\hat{P}\times\hat{P})\mathrm{Re}(\rho+\hat{P}\times\rho)_{+-}$ also has a double zero from the second term which is due to the absorption. This mechanism for production of this double zero is similar to that of HK, although the real part of the Pomeron utilized therein vanishes because of a Bessel function zero at $t\approx -0.5$. Figure 16 also shows that the P'' pole plays a role only in the elastic phases near $t=0$. It is conceivable that it could be eliminated entirely (and certainly changed) in models with slightly different assumptions, e.g., including $\hat{P}\times\hat{P}\times\hat{P}$ cuts or more complicated pole residue functions.

The size and phase of the absorptive corrections to secondary pole terms are illustrated in Fig. 18, where the absorbed and unabsorbed ρ and A_2 poles in K^-p elastic scattering at $t=-0.05$ GeV^2, $p=10$ GeV/c are plotted. The advertised features of the absorption are clear. The imaginary helicity-nonflip vector pole is absorbed more than its real part (so the forward $\pi^- p\to\pi^0 n$ differential cross section which samples both $\mathrm{Re}M_{++}^{I=1}$ and $\mathrm{Im}M_{++}^{I=1}$ decreased faster than $\Delta\sigma_{\mathrm{tot}}^{\pi^\pm p}$). The helicity-flip vector pole is absorbed less than the nonflip, as in any absorption model, so the integrated $\pi^- p\to\pi^0 n$ differential cross section decreases faster yet. Figure 18 also shows that the absorption for the A_2 pole is like that of the ρ pole when the real and imaginary parts are interchanged, although due to the less peripheral A_2 pole the tensor helicity-flip absorption is more pronounced than the vector flip absorption. This is the same picture as in HK.[2]

One of the most interesting points is the description of the flat shape of $\sigma_{\mathrm{tot}}^{K^+p}$ (see Fig. 1). Figure 19 shows the $t=0$ nonflip absorbed and unabsorbed K^+p elastic amplitudes at 10 GeV/c. The large negative $\hat{P}\times\hat{P}$ and $\omega+\hat{P}\times\omega$ terms drop off faster than the $\hat{P}$ pole and yield a flat total K^+p cross section up to our cutoff energy of ~30 GeV/c. As we have mentioned, Pomeron renormalization effects are presumably responsible for the flatness, or even slight increase of $\sigma_{\mathrm{tot}}^{K^+p}$ beyond 30 GeV/c. It is also clear that the ρ and A_2 terms play minor roles in this behavior, and the P'' plays no role at all. It is well to remember in contrasting this rather complex mechanism with the simple mechanism of unabsorbed exchange-degenerate poles plus a simple Pomeron pole with unit intercept that the latter simple mechanism also predicts that the $t=0$ real-to-imaginary K^-p elastic amplitude ratio vanishes. Experimentally this quantity is not zero, and appears to be in qualitative agreement with our description (see Fig. 2).

The question of the extent to which our results do exhibit exchange degeneracy will now be considered As we have stated, although we have not assumed intercept exchange degeneracy nor wrong-signa-

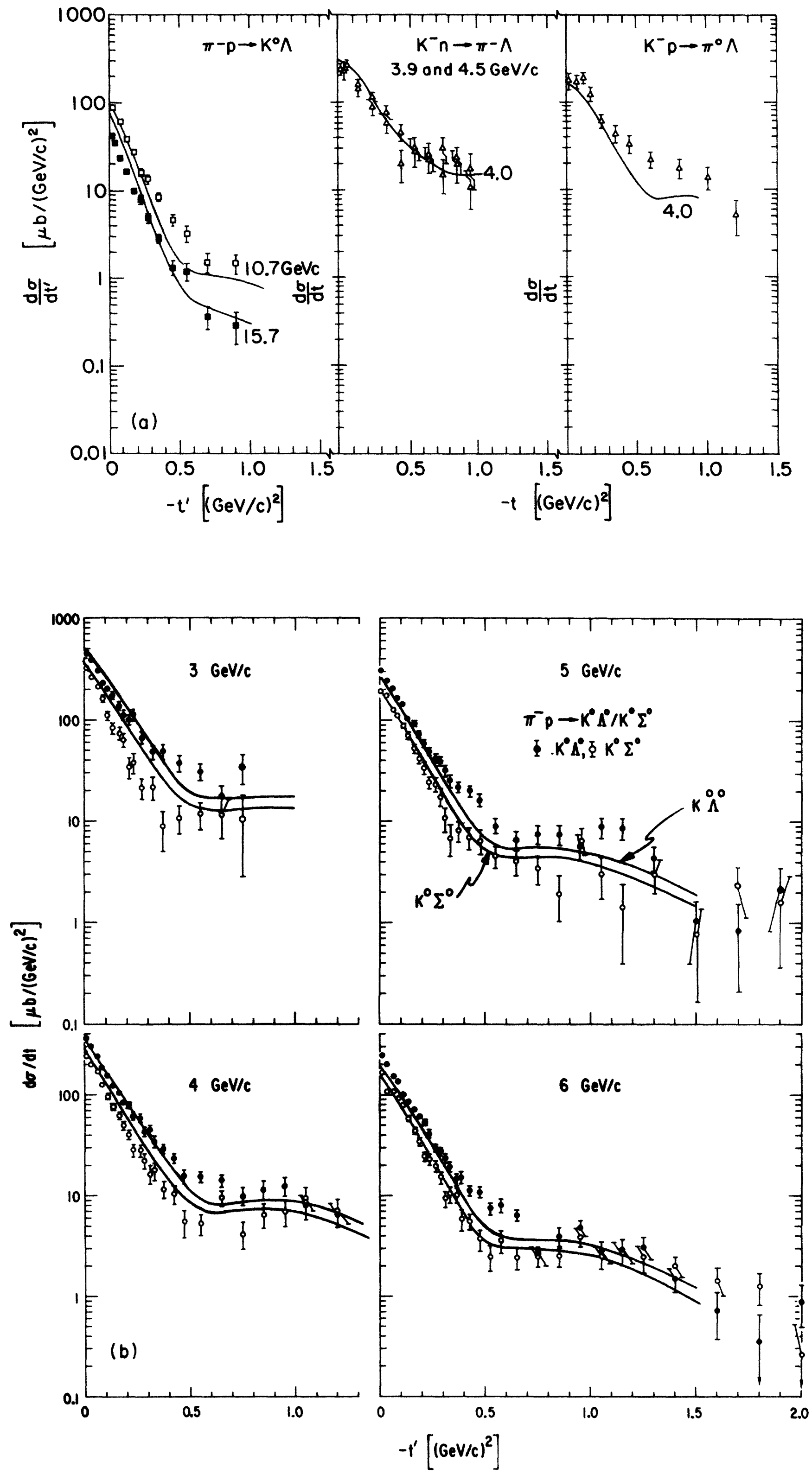

FIG. 13. (a) Hypercharge-exchange differential cross sections: $\pi^- p \to K^0\Lambda$, $K^- n \to \pi^-\Lambda$, and $K^- p \to \pi^0\Lambda$. (b) Low-energy $\pi^- p \to K^0\Sigma^0$ and $\pi^- p \to K^0\Lambda^0$ differential cross sections.

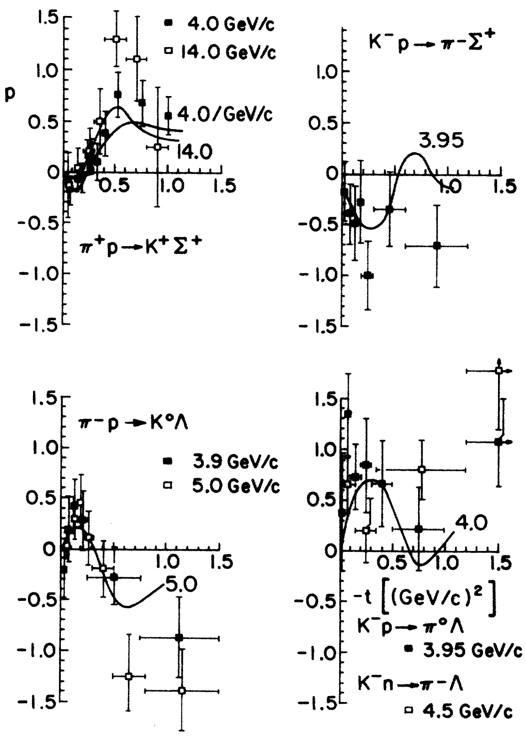

FIG. 14. Hypercharge-exchange polarizations: $\pi^+p \to K^+\Sigma^+$, $\pi^-p \to K^0\Lambda$, $K^-p \to \pi^-\Sigma^+$, $K^-p \to \pi^0\Lambda$, and $K^-n \to \pi^-\Lambda$.

ture nonsense zeros, our secondary poles do have a remarkable exchange-degenerate set of $t=0$ couplings as is evident from Table II. This is true for both helicity-flip and -nonflip couplings. Moreover, the total (pole + cut) flip amplitudes exhibit

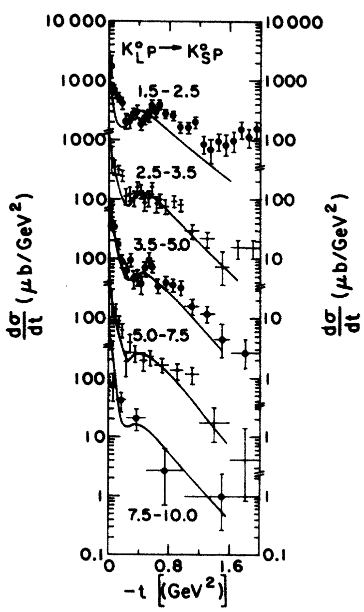

FIG. 15. Differential cross sections for $K^0_L p \to K^0_S p$.

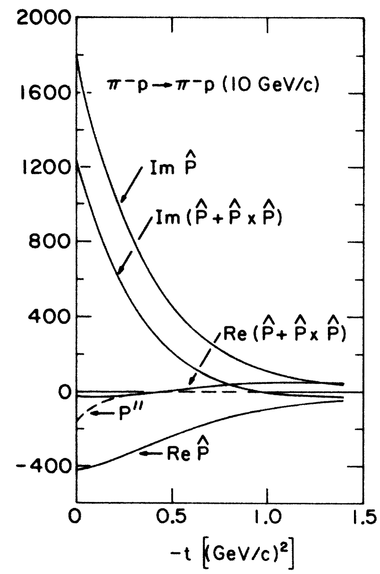

FIG. 16. Isoscalar helicity-nonflip amplitudes at 10 GeV/c for $\pi^-p \to \pi^-p$. The unabsorbed and absorbed $\hat{P}$ pole are shown along with the $J=0$ vacuum pole P''.

a large measure of exchange-degenerate behavior, as they do in HK's treatment. Figures 3 and 17 show the $\pi^-p \to \pi^0 n$ amplitudes in Halzen's and Michael's notation and in our notation. The "wrong-signature nonsense zero"-like result of a double zero in ReM^{ρ}_{+-} and a single zero in ImM^{ρ}_{+-} at $t \approx -0.5$ are reproduced in our absorbed amplitudes. The corresponding results for tensor exchange having no zero in Re$M^{A_2}_{+-}$ and a single zero in Im$M^{A_2}_{+-}$ at $t \approx -0.5$ are also reproduced by our absorption (see Fig. 20). The peripheral nature of ImM^{ρ}_{++} with the crossover zero at $t=-0.2$

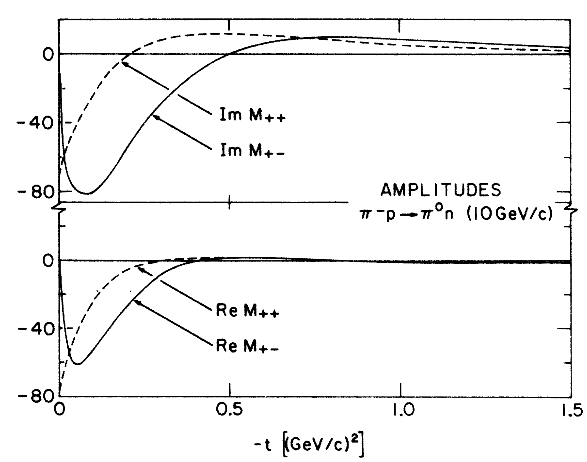

FIG. 17. Amplitudes for $\pi^-p \to \pi^0 n$ at 10 GeV/c.

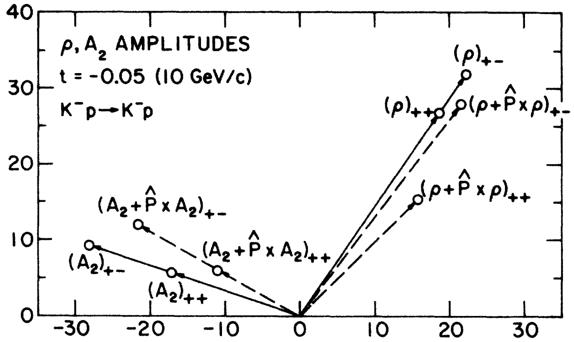

FIG. 18. Unabsorbed and absorbed ρ and A_2 amplitudes at 10 GeV/c, $t = -0.05$ (GeV/c)^2 for $K^-p \to K^-p$. Note the stronger absorption of Im(ρ) and Re(A_2) relative to Re(ρ) and Im(A_2), respectively, due to the phase of the bare Pomeron pole.

(GeV/c)^2 is a direct result of the absorption in the nonflip imaginary ρ amplitude; ReM^{ρ}_{++} is absorbed less and does not have this peripheral zero. The essential exchange-degenerate character of the secondary flip amplitudes is also apparent from a glance at Figs. 21 and 22 in which the amplitudes for the "rotating" $K^-p \to \bar{K}^0n$ and "real" $K^+n \to K^0p$ reactions at 10 GeV/c are plotted. The "rotating" flip amplitude does indeed rotate as in an unab-

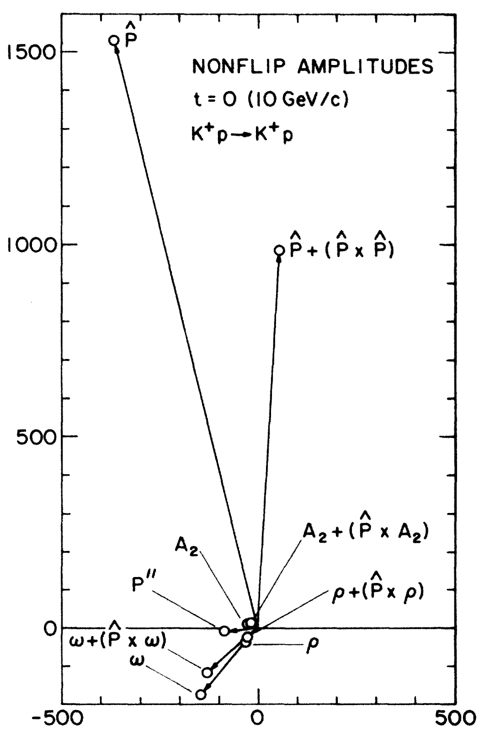

FIG. 19. Helicity-nonflip $t = 0$ $K^+p \to K^+p$ amplitudes at 10 GeV/c showing relative contributions to $\sigma_{\rm tot}^{K^+p}$.

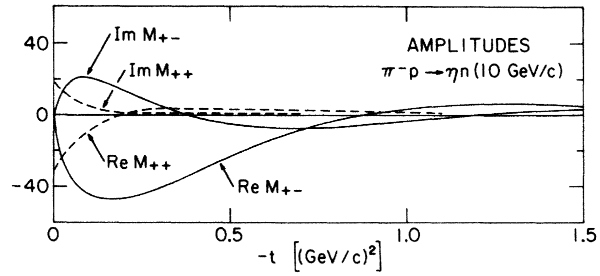

FIG. 20. Amplitudes for $\pi^-p \to \eta n$ at 10 GeV/c.

sorbed exchange-degenerate pole model. The "real" amplitudes are indeed mainly real, but have a 25% imaginary component. The corresponding differential cross sections and polarizations are shown in Figs. 10 and 11. The "real" pole term is larger than the "rotating" pole term, and absorption brings the two closer together.[2]

The corresponding results for the hypercharge-exchange reactions are similar though exchange degeneracy is broken somewhat more than in the $A_2 \pm \rho$ reactions. Figures 23 and 24 show the 10-GeV/c amplitudes for the line-reversed pair of reactions $\pi^+p \to K^+\Sigma^+$ and $K^-p \to \pi^-\Sigma^+$. The "rotating" flip amplitude does rotate to a significant extent, but the "real" flip amplitude has comparable imaginary and real parts (although the "real" nonflip amplitude is mostly real). All this is in agreement with the hypercharge polarizations and cross sections as shown in Figs. 12–14. It should be remembered that these fits were performed with the K^* and K^{**} intercepts equal to the ρ and A_2

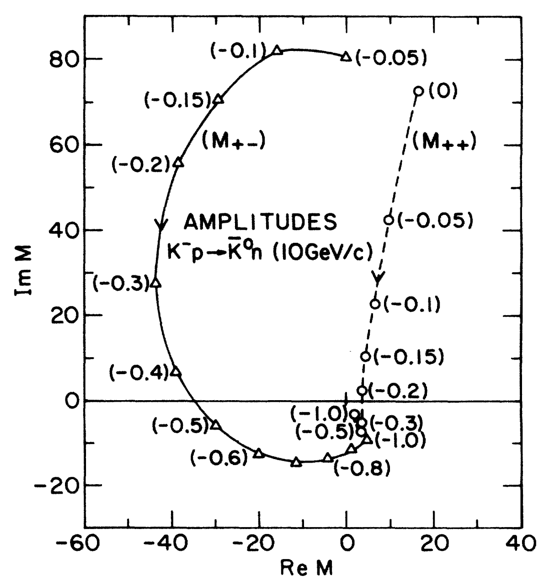

FIG. 21. The "rotating" $K^-p \to \bar{K}^0n$ amplitude at 10 GeV/c. Values of t in (GeV/c)^2 are given in parentheses.

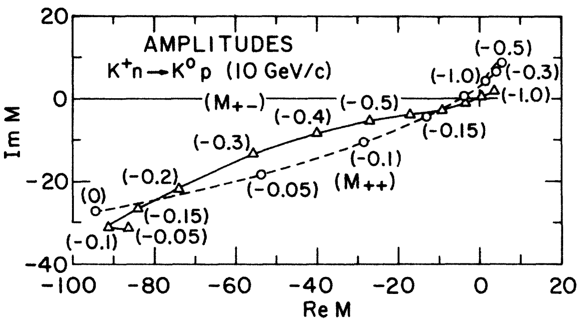

FIG. 22. The "real" amplitude $K^+n \rightarrow K^0p$ at 10 GeV/c.

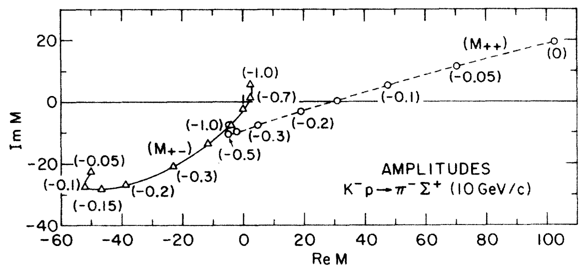

FIG. 24. The "real" hypercharge-exchange amplitudes for $K^-p \rightarrow \pi^-\Sigma^+$ at 10 GeV/c.

intercepts, respectively. Breaking this constraint would undoubtedly lead to better results in some of the details.

Finally, we consider the reaction $K_L^0 p \rightarrow K_S^0 p$ (see Fig. 15). This reaction is controlled by $-(\omega + \hat{P}\times\omega)$ near $t=0$, as shown by regeneration phase measurements[45] which show this phase φ to be $\varphi \simeq -135° \pm 20°$. Our results at 10 GeV/$c$ give $\varphi = -138°$. The SU(3) predictions relating to ω- and ρ-pole contributions are in our notation[44]

$$\tilde{\beta}^{\omega}_{s,f} = (4F_{+\pm} - 1)\,\tilde{\beta}^{\rho}_{s,f} \ ,$$

$$\gamma^{\omega}_{s,f} = \gamma^{\rho}_{s,f} \ .$$

The nonflip relation is actually well satisfied with our pole parametrizations and our value $F_{++} = 1.6$. The flip relation is broken since we obtain $F_{+-} = 0.18$ and we have set $\tilde{\beta}^{\omega}_{f} = 0$, but the breaking is not severe. We should emphasize that this SU(3) relation implies that $\Delta\sigma^{K^\pm p}_{\text{tot}}$ and $\Delta\sigma^{\pi^\pm p}_{\text{tot}}$ fall off at the same rate since the ω and ρ absorptions are then in the same proportions. This is almost the case, the difference in the rate of falloffs being $s^{0.08}$, which varies ~10% between 5 and 20 GeV/c. A glance at our total cross section fit (Fig. 1) shows our results are reasonable.

For completeness, we show the b-space projections of the bare Pomeron and the $\pi^-p \rightarrow \pi^0 n$ and $\pi^-p \rightarrow \eta n$ amplitudes in Figs. 25–29. We shall not enter into any detailed discussion of these results, as they are equivalent to the discussion already given. Some comments are included in the figure captions. The projections of the absorbed ρ and A_2 amplitudes are similar to HK's and the discussion there is also applicable to our results.[46] The b-space bare Pomeron projection is somewhat different in the two approaches, but is qualitatively the same.

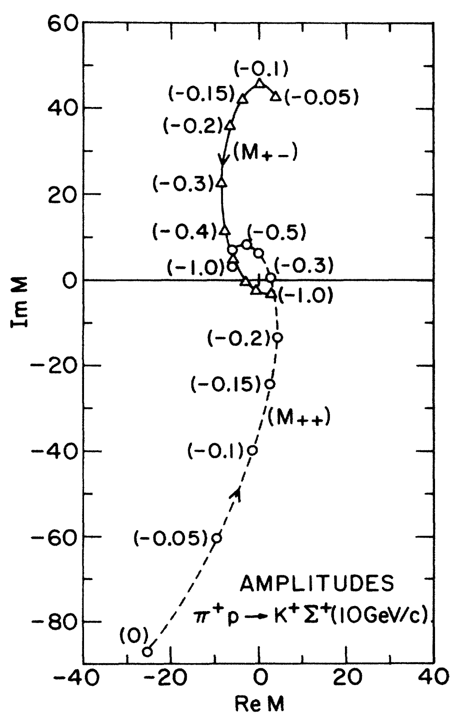

FIG. 23. The "rotating" hypercharge-exchange amplitudes for $\pi^+p \rightarrow K^+\Sigma^+$ at 10 GeV/c.

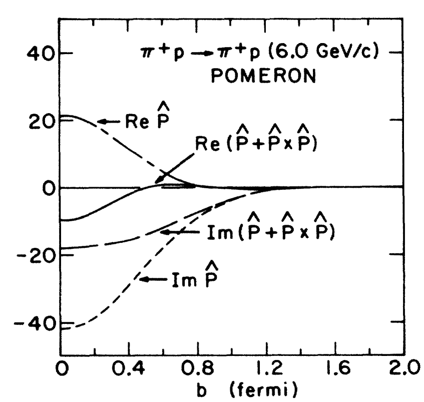

FIG. 25. b-space projections of the unabsorbed and absorbed bare Pomeron pole $\hat{P}$ at 6 GeV/c. Note the dominant central Gaussian-like feature in the absorbed $\hat{P}$ with a significant "edge" effect at $b \approx 1$ F. (1 F $\approx$ 5 GeV^{-1} or $J_s \approx 7.5$.) The "edge" appears naturally, and is not added in by hand.

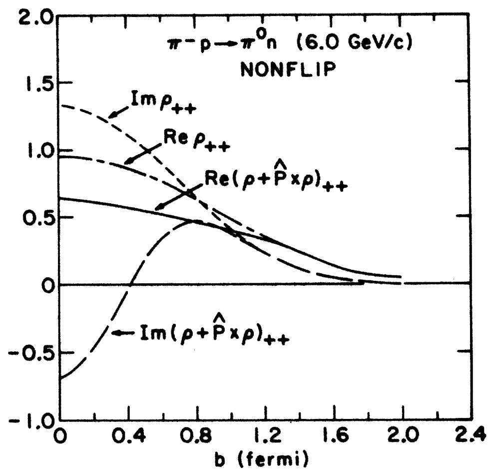

FIG. 26. Helicity-nonflip b-space amplitudes for $\pi^- p \to \pi^0 n$ at 6 GeV/c. Note the peripheral nature of $\mathrm{Im}(\rho + \hat{P} \times \rho)_{++}$ and the nonperipheral real part.

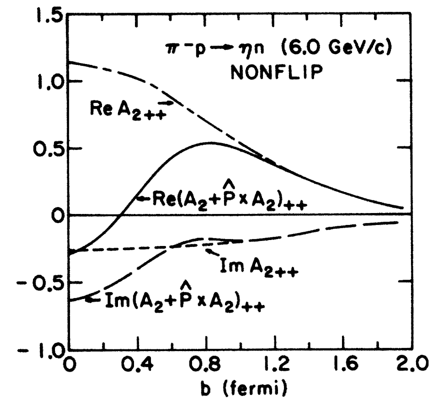

FIG. 28. Helicity-nonflip b-space amplitudes for $\pi^- p \to \eta n$ at 6 GeV/c. Note the peripheral real part of $(A_2 + \hat{P} \times A_2)_{++}$ relative to its imaginary part, as contrasted with the case for ρ exchange.

V. CONCLUSIONS

We have succeeded in obtaining a very reasonable global fit to a very considerable set of $0^-\frac{1}{2}^+ \to 0^-\frac{1}{2}^+$ data in the intermediate-energy range. We cannot claim uniqueness, and thus the success of our fit is no proof that the notion of an unrenormalized Pomeron is a powerful one, but we believe that the fit is graceful and not too strained, and this gives a measure of plausibility to our idea. In general, all of our fits to differential cross sections are quite reasonable up to $|t| \approx 0.7$ (GeV/$c)^2$, and begin to deviate beyond that point. There are many explanations for this. Probably the two most obvious ones are the rather naive structure of our residues and the primitive sort of absorption used throughout. The polarization curves also engage in mild gyrations at some spots, but since they are far more sensitive to delicate phase relations the result is not unexpected. Perhaps a bit more disturbing is the fact, shared with some absorption models, that the large-$|t|$ region shrinkage is not accurately described. This is particularly evident in the charge-exchange reactions and it could be due to several defects of our parametrization, among which the two previously mentioned play an important role. On the whole, however, we believe that the fit is a reasonable one.

It is clear from the description of the amplitudes used, that we have made a number of very specific choices with regard to trajectories including absorption prescriptions, absence of wrong-signature zeros, our form of exchange degeneracy, etc. It is not clear to us that we have made the correct choice in any of the above matters, and we would not find it surprising that a very respectable de-

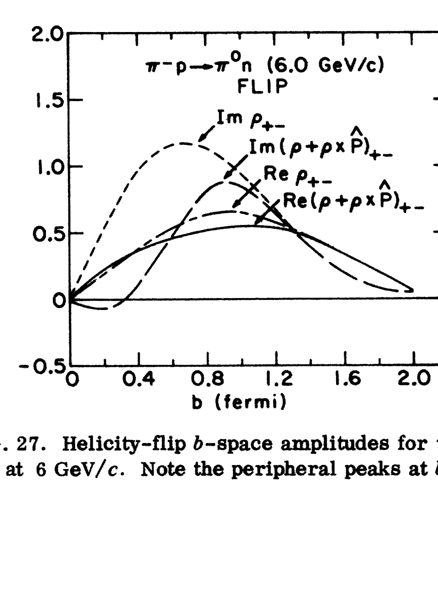

FIG. 27. Helicity-flip b-space amplitudes for $\pi^- p \to \pi^0 n$ at 6 GeV/c. Note the peripheral peaks at $b \approx 1$ F.

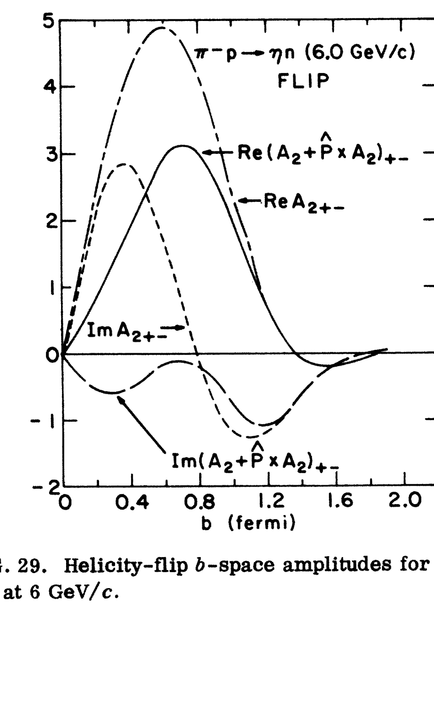

FIG. 29. Helicity-flip b-space amplitudes for $\pi^- p \to \eta n$ at 6 GeV/c.

scription of the data could be achieved with different choices in many of them. We are also aware that our description does involve many more or less independent parameters.[14] However, not being professional phenomenologists, we do not pretend to be settling any issues with our fit, but rather making a particular point of view about the nature of diffraction plausible, so we do not consider this criticism excessively serious. A more serious point is the fact that no attempt was made to include any nucleon-nucleon data to which our fit is intimately connected through factorization. Nucleon-nucleon phenomenology is a science unto itself, and at this time we lack the machinery and manpower to carry out such an ambitious program, but we expect it will be done in the near future, and we have no reason to believe it will not succeed.

In assessing the results we have obtained, it is important to keep the objectives of the exercise clearly in focus. These are concerned with a direct attempt to utilize multiparticle phenomenology and unitarity to construct the nature of diffraction scattering in two-body processes. The consistency of the approach in turn leads to statements about the nature of inelastic diffraction in multiparticle events. The critical point revolves around the concept of the single-fireball cross section σ_{sf} which is assumed to comprise enough of the total inelastic cross section at intermediate energies to determine its leading-power behavior, which is called the bare Pomeron intercept minus one. It is clear that all these concepts are nebulous unless substantial examination of inelastic data is carried out. We have already indicated the beginning of such a program, which has comprised, among other things, examination of triple-Regge data[11] and maximum-rapidity-gap distributions[12] as well as the possibility of utilizing the resonance ABFST model as at least a first approximation to σ_{sf}.[13,14] Further study along these lines in parallel with further examination of two-body data would be highly desirable.

ACKNOWLEDGMENTS

We would like to thank Professor G. Kane for many valuable discussions, and Dr. P. D. B. Collins for making available to us part of his compilation of two-body scattering data. One of us (JD) wished to thank the University of Washington for its generous hospitality during which the bulk of this work was performed.

APPENDIX

In this appendix we give the parametrization and formalism used in the text.

Our normalization is

$$\sigma_{\text{tot}}^{ab}(\text{mb}) = \frac{0.389}{\lambda^{1/2}(s, m_a^2, m_b^2)} \operatorname{Im} M_{++}^{ab\to ab}(s,0) \tag{A1}$$

$$\frac{d\sigma}{dt}(\text{mb/GeV}^2) = \frac{0.389}{16\pi\lambda(s, m_a^2, m_b^2)} \times (|M_{++}|^2 + |M_{+-}|^2)\,, \tag{A2}$$

$$P = \frac{-2\operatorname{Im}(M_{++}M_{+-}^*)}{|M_{++}|^2 + |M_{+-}|^2}\,. \tag{A3}$$

For $\pi^- p \to (\eta \to 2\gamma) n$ we multiply Eq. (2) by the $\eta \to 2\gamma$ branching ratio.

Our second-order-cut formula (with $\lambda = 1$) for the convolution of two poles is

$$(\text{cut})_{+\pm} = \frac{i}{8\pi^2 \lambda^{1/2}(s, m_a^2, m_b^2)} \int \frac{dt_1 dt_2}{|\lambda^{1/2}(t, t_1, t_2)|} \left[\delta_{n0} + \frac{t_2 - t_1 - t}{2(tt_1)^{1/2}}\,\delta_{n1}\right] * [(\text{pole})_{++}(\text{pole})_{+\pm}]\,, \tag{A4}$$

with $n = 0, 1$ for nonflip, flip. Notice that our formula for $\hat{P}\times\hat{P}$ cuts is defined not to have a factor (1/2!). It is therefore not being treated as in the eikonal model,[1] but rather with a K-matrix prescription.

We write the pole terms contributing to reaction i denoted by $a_i\, b_i \to c_i\, d_i$ as

$$(\text{pole})_{++}^{ki} = \tau_k\, \beta_s^{ki}\, e^{\gamma_s^k t} \left(e^{-i\pi/2} \frac{s}{s_0}\right)^{\alpha_k(t)}\,, \tag{A5}$$

$$(\text{pole})_{+-}^{ki} = \sqrt{-t}\;\tau_k\, \beta_f^{ki}\, e^{\gamma_f^k t} \left(e^{-i\pi/2} \frac{s}{s_0}\right)^{\alpha_k(t)}\,, \tag{A6}$$

where $k = 1, \ldots, 7$ corresponds to $\hat{P}$, P'', ω, ρ, A_2, K^*, and K^{**}, and $\tau_k = \left\{{-1 \atop i}\right\}$ for $\{\pm\}$ signature. The cut term for reaction i for the kth pole is calculated as the second-order $\hat{P}\times(\text{pole})^{ki}$ cut multiplied by λ factors as follows:

$$(\text{cut})_{++}^{ki} = -i\lambda_{ki}\, \tau_k\, \beta_s^{ki}\, \beta_s^{\hat{P}i} \left(e^{-i\pi/2} \frac{s}{s_0}\right)^{\alpha_k^0 + \alpha_{\hat{P}}^0} \times e^{\Gamma_s^k t} (\mathfrak{F}_+^{ki})^{-1}\,, \tag{A7}$$

$$(\text{cut})_{+-}^{ki} = -i\sqrt{-t}\;\lambda_{ki}\, \tau_k\, \beta_f^{ki}\, \beta_s^{\hat{P}i} \left(e^{-i\pi/2} \frac{s}{s_0}\right)^{\alpha_k^0 + \alpha_{\hat{P}}^0} \times e^{\Gamma_f^k t} (\mathfrak{F}_-^{ki})^{-1}\,, \tag{A8}$$

where

$$\Gamma_s^k(s) = x_s^k x_s^{\hat{P}}(x_s^k + x_s^{\hat{P}})^{-1} , \quad (A9)$$

$$\Gamma_f^k(s) = x_f^k x_s^{\hat{P}}(x_f^k + x_s^{\hat{P}})^{-1} , \quad (A10)$$

$$x_{s,f}^k(s) = \gamma_{s,f}^k + \alpha_k' \ln(e^{-i\pi/2} s/s_0) , \quad (A11)$$

$$\mathfrak{F}_+^{ki}(s) = 8\pi\lambda^{1/2}(s, m_{ai}^2, m_{bi}^2)(x_s^k + x_s^{\hat{P}}), \quad (A12)$$

$$\mathfrak{F}_-^{ki}(s) = 8\pi\lambda^{1/2}(s, m_{ai}^2, m_{bi}^2) \times (x_f^k + x_s^{\hat{P}})^2 (x_s^{\hat{P}})^{-1} . \quad (A13)$$

For hypercharge reactions, we replace t by $t - t_{\min}$ everywhere. Since $|t_{\min}| < 0.03$ even at $p_{\text{lab}} = 3$ GeV/c, this is a small effect. The amplitudes M_{++}^i for reaction i are then

$$M_{+\pm}^i = \sum_{k=1}^{7} [(\text{pole})_{+\pm}^{ki} + (\text{cut})_{+\pm}^{ki}] . \quad (A14)$$

The parameters β_s^{ki}, β_f^{ki}, and λ_{ki} are defined as follows. For the bare Pomeron $\hat{P}$ we introduce SU(3) breaking factors $\hat{S}_\pi$ and $\hat{S}_K$ for the $\hat{P}$ contribution to πN and KN elastic scattering so that

$$\beta_s^{\hat{P}i} = \begin{Bmatrix} \hat{S}_\pi \\ \hat{S}_K \end{Bmatrix} \beta_s^{\hat{P}} \text{ for } i = \begin{Bmatrix} \pi N \text{ elastic} \\ KN \text{ elastic} \end{Bmatrix} . \quad (A15)$$

The helicity-flip isoscalar amplitude is set equal to zero so that $\tilde{\beta}_f^{\hat{P}} = 0$. For $\hat{P} \times \hat{P}$ cuts we have two λ factors, again for πN and KN elastic scattering:

$$\lambda_{\hat{P}i} = \begin{Bmatrix} \lambda_{\hat{P}\pi} \\ \lambda_{\hat{P}K} \end{Bmatrix} \text{ for } i = \begin{Bmatrix} \pi N \text{ elastic} \\ KN \text{ elastic} \end{Bmatrix} . \quad (A16)$$

We set $\lambda_{P''i} = 0$ (no $\hat{P} \times P''$ cuts). For $\hat{P} \times R^k$ cuts ($R^k = \omega, \rho, A_2, K^*, K^{**}$) we take

$$\lambda_{ki} = \begin{Bmatrix} (\hat{S}_\pi)^{-1} \\ (\hat{S}_K)^{-1} \end{Bmatrix} \text{ if the beam particle for reaction } i \text{ is } \begin{Bmatrix} \pi \\ K \end{Bmatrix} . \quad (A17)$$

This corresponds to the ordering $\hat{P} \times R$. For the ordering $R \times \hat{P}$ we must replace the beam meson by the final meson. Since $\beta_s^{\hat{P}i}$ has factors $\{\begin{smallmatrix}\hat{S}_\pi \\ \hat{S}_K\end{smallmatrix}\}$, all cuts are numerically independent of $\hat{S}_\pi$ and $\hat{S}_K$. The cuts using the ordering $\hat{P} \times R$ via Eqs. (A7) and (A8) are the same as would be calculated by the $\sqrt{S} \times R \times \sqrt{S}$ Sopkovich prescription. With, e.g., $\pi N \to K\Sigma$, the λ factor $\hat{S}_\pi^{-1}$ would be applied to the initial $\frac{1}{2}\hat{P} \times R$ absorption which has a factor $\hat{S}_\pi$ from $\hat{P}$, and a factor $\hat{S}_K^{-1}$ is applied to the final $\frac{1}{2}R \times \hat{P}$ absorption which has a factor $\hat{S}_K$. As we have said, all the λ_{ki} parameters are less than 1 in our approach. For an eikonal unitarization of the $\hat{P}$ the λ factors for $\hat{P} \times \hat{P}$ cuts should be multiplied by 2. All other λ factors remain unchanged.

The parameters β_s^{ki} and β_f^{ki} are found by multiplying the SU(3) coefficients in Table I by the numbers in Table II. That is, for reaction i and pole k,

$$\beta_{s,f}^{ki} = (\text{coefficient in Table I})_{ki} \; (\tilde{\beta}_{s,f}^k \text{ in Table II}) , \quad (A18)$$

where (s, f) refer to (nonflip, flip).

Finally, the transition to b space is made through the following formula with $n = (0, 1)$ referring to (nonflip, flip):

$$\tilde{M}_{+\pm}(s, b) = -\frac{2s}{\lambda(s, m_a^2, m_b^2)} \times \int_0^\infty M_{+\pm}(s, t) J_n(b\sqrt{-t}) \sqrt{-t}\, d(\sqrt{-t}). \quad (A19)$$

If, as is true in our approach,

$$M(s, t) = \sum_j A_j (-t)^{n/2} e^{k_j t} \quad (A20)$$

then we get the simple result

$$\tilde{M}(s, b) = -\sum_j \frac{A_j b^n}{(2k_j)^{n+1}} (e^{-b^2/4k_j}) \frac{2s}{\lambda(s, m_a^2, m_b^2)} . \quad (A21)$$

*Work performed under the auspices of the U. S. Atomic Energy Commission.

[1] R. C. Arnold, Phys. Rev. 153, 1523 (1967); R. C. Arnold and M. L. Blackmon, *ibid.* 176, 2082 (1968); F. Henyey, G. L. Kane, J. Pumplin, and M. Ross, *ibid.* 182, 1579 (1969); G. Cohen-Tannoudji, A. Morel, and H. Navelet, Nuovo Cimento 40, 1074 (1967); K. G. Boreskov, A. M. Lapidus, S. T. Sukhorukhov, and K. A. Ter-Martirosyan, Nucl. Phys. B40, 307 (1972). For a review, see R. J. N. Phillips, CERN Report No. 72/17, 1972 (unpublished); G. C. Fox and C. Quigg, Annu. Rev. Nucl. Sci. 23, 219 (1973).

[2] B. J. Hartley and G. L. Kane, Nucl. Phys. B57, 157 (1973); G. Kane, in *Particles and Fields—1973*, pro-

ceedings of the Berkeley Meeting of the Division of Particles and Fields of the APS, edited by H. H. Bingham, M. Davier, and G. R. Lynch (A.I.P., New York, 1973).

[3]A. Martin and P. R. Stevens, Phys. Rev. D 5, 147 (1972); 8, 2076 (1973).

[4]G. A. Ringland, R. G. Roberts, D. P. Roy, and J. Tran Thanh Van, Nucl. Phys. B44, 395 (1972); D. Barkai and K. J. M. Moriarty, *ibid.* B50, 354 (1972).

[5]N. Barik and B. R. Desai, Phys. Rev. D 6, 3192 (1972).

[6]V. Barger and R. J. N. Phillips, Phys. Rev. 187, 2210 (1969).

[7]H. Harari, Phys. Rev. Lett. 26, 1400 (1971); Ann. Phys. (N.Y.) 63, 432 (1971).

[8]J. S. Loos and J. A. J. Matthews, Phys. Rev. D 6, 2463 (1973).

[9]F. Henyey, R. Hong Tuan, and G. L. Kane, Nucl. Phys. B70, 445 (1974).

[10]G. F. Chew, in *High Energy Collisions—1973*, proceedings of the fifth international conference on high energy collisions, Stony Brook, 1973, edited by C. Quigg (A.I.P., New York, 1973); UCB Report No. LBL-2174, 1973 (unpublished); M. Bishari, G. F. Chew, and J. Koplik, Nucl. Phys. B72, 61 (1974); G. F. Chew, T. Rogers, and D. R. Snider, Phys. Rev. D 2, 765 (1970).

[11]J. W. Dash, Phys. Rev. D 9, 200 (1974).

[12]J. W. Dash, Phys. Lett. 49B, 81 (1974).

[13]J. Dash, J. Huskins, and S. T. Jones, Phys. Rev. D 9, 1404 (1974); J. Dash and S. T. Jones, *ibid.* 9, 2539 (1974).

[14]J. Dash, G. Parry, and M. Grisaru, Nucl. Phys. B53, 91 (1973). Recent work indicates that the ABFST model is also capable of generating the qualitative features of the t dependence of the bare Pomeron residue and trajectory function used here. See J. Dash and S. Jones, ANL Reports Nos. ANL/HEP 7422 and 7429, 1974 (unpublished).

[15]A preliminary account of this work is contained in N. F. Bali and J. W. Dash, ANL Report No. ANL/HEP 7372, rev., 1973 (unpublished).

[16]K. A. Ter-Martirosyan, Phys. Lett. 44B, 179 (1973).

[17]L. Caneschi, Phys. Rev. Lett. 23, 254 (1969); J. Dash, J. R. Fulco, and A. Pignotti, Phys. Rev. D 1, 3164 (1970).

[18]G. F. Chew and D. R. Snider, Phys. Lett. 31B, 75 (1970).

[19]V. N. Gribov, Zh. Eksp. Teor. Fiz. 53, 654 (1967) [Sov. Phys.—JETP 26, 414 (1968)].

[20]J. Ng and U. P. Sukhatme, Nucl. Phys. B55, 253 (1973).

[21]G. F. Chew and D. R. Snider, Phys. Rev. D 1, 3453 (1970); 3, 420 (1971).

[22]See, e.g., A. Capella, Phys. Rev. D 8, 2047 (1973).

[23]See, e.g., A. Capella, M. S. Chen, M. Kugler, and R. Peccei, Phys. Rev. Lett. 31, 497 (1973).

[24]The $J\approx 0$ vacuum pole P'' was taken to have a free intercept in the fitting program to allow for the possibility of an unrenormalized P' in addition to the $\hat{P}$. Its SU(3) properties were consequently taken as that of the P' in performing the fit. The SU(3) properties of the unrenormalized vacuum trajectories in any case are expected to change upon renormalization.

[25]W. Galbraith *et al.*, Phys. Rev. 138, B913 (1965); W. F. Baker *et al.*, Phys. Rev. 129, 2285 (1967); K. J. Foley *et al.*, Phys. Rev. Lett. 19, 330 (1967); S. P. Denisov *et al.*, Phys. Lett. 36B, 415 (1971); *ibid.* 36B, 528 (1971).

[26]K. J. Foley *et al.*, Phys. Rev. 181, 1775 (1969); U. Amaldi, conference talk given at the Second International Conference on Elementary Particles, Aix-en-Provence, 1973 (unpublished); Data Compilation CERN Report No. CERN/HERA 69-3 (unpublished); J. R. Campbell *et al.*, Nucl. Phys. B64, 1 (1973).

[27]F. Halzen and C. Michael, Phys. Lett. 36B, 367 (1971).

[28]S. Brandt *et al.*, Phys. Rev. Lett. 10, 413 (1963); K. J. Foley *et al.*, *ibid.* 11, 425 (1963); C. T. Coffin *et al.*, Phys. Rev. 159, 1169 (1967); D. R. Rust *et al.*, Phys. Rev. Lett. 24, 1361 (1970); Yu. M. Antipov *et al.*, in *Proceedings of the Fourth International Conference on High Energy Collisions, Oxford, 1972*, edited by J. R. Smith (Rutherford High Energy Laboratory, Chilton, Didcot, Berkshire, England, 1972), p. 230.

[29]K. J. Foley *et al.*, Phys. Rev. Lett. 11, 503 (1963); W. De Baere *et al.*, Nuovo Cimento 45A, 885 (1966); J. Mott *et al.*, Phys. Lett. 23, 171 (1966); M. Aderholz *et al.*, *ibid.* 24, 434 (1967); R. J. Miller *et al.*, *ibid.* 34B, 230 (1971); Yu. M. Antipov *et al.*, in *Proceedings of the Fourth International Conference on High Energy Collisions, Oxford, 1972*, edited by J. R. Smith (Rutherford High Energy Laboratory, Chilton, Didcot, Berkshire, England, 1972), p. 230.

[30]M. Borghini *et al.*, Phys. Lett. 31B, 405 (1970); CERN report, 1972 (unpublished).

[31]A. V. Stirling *et al.*, Phys. Rev. Lett. 14, 763 (1965); P. Sonderegger *et al.*, Phys. Lett. 20, 75 (1966); O. Guisan *et al.*, *ibid.* 18, 200 (1965); K. Ruddick *et al.*, private communication to G. Kane.

[32]D. D. Drobnis *et al.*, Phys. Rev. Lett. 20, 274 (1968); P. Bonamy *et al.*, Nucl. Phys. B16, 335 (1970); Ref. 23; D. Hill *et al.*, Phys. Rev. Lett. 30, 239 (1973).

[33]P. Astbury *et al.*, Phys. Lett. 23, 396 (1966); D. Cline *et al.*, University of Wisconsin report, 1969 (unpublished); Phys. Rev. Lett. 23, 1318 (1969); A. Firestone *et al.*, *ibid.* 25, 958 (1970); M. Haguenauer *et al.*, Phys. Lett. 37B, 538 (1971).

[34]E. H. Willen *et al.*, paper contributed to the Fourth International Conference on High Energy Collisions, Oxford, 1972.

[35]W. Beusch *et al.*, CERN report, 1973 (unpublished).

[36]S. M. Pruss *et al.*, Phys. Rev. Lett. 23, 189 (1969).

[37]A. Bashian *et al.*, Phys. Rev. D 4, 2667 (1971).

[38]P. Kalbaci *et al.*, Phys. Rev. Lett. 27, 74 (1971).

[39]L. Moscoso *et al.*, Nucl. Phys. 36B, 332 (1972).

[40]D. Birnbaum *et al.*, Phys. Lett. 31B, 484 (1970).

[41]C. E. Ward *et al.*, Phys. Rev. Lett. 31, 1149 (1973); 32, 264(E) (1974).

[42]C. E. W. Ward *et al.*, Argonne report, 1971 (unpublished); W. L. Yen *et al.*, Phys. Rev. 188, 2011 (1969); M. Abramovich *et al.*, Nucl. Phys. B27, 477 (1971).

[43]G. W. Brandenburg *et al.*, Phys. Rev. D 9, 1939 (1974).

[44]J. A. J. Matthews, SLAC Report No. 1313, 1973 (unpublished).

[45]D. Freytag *et al.*, and R. F. Albrecht *et al.*, papers contributed to the Second International Conference on Elementary Particles, Aix-en-Provence, 1973 (unpublished).

[46]See also P. R. Stevens, Phys. Rev. D 9, 1425 (1974).